

Available online at www.sciencedirect.com

ScienceDirect

<http://www.elsevier.com/locate/biombioe>

Experimental study and characterization of a two-compartment cylindrical internally circulating fluidized bed gasifier

J.P. Simanjuntak^{a,b}, Z.A. Zainal^{a,*}

^a School of Mechanical Engineering, Universiti Sains Malaysia, Engineering Campus, Nibong Tebal 14300, Penang, Malaysia

^b Mechanical Engineering Department, State University of Medan, Medan 20221, North Sumatera, Indonesia

ARTICLE INFO

Article history:

Received 19 November 2013

Received in revised form

16 January 2015

Accepted 20 March 2015

Available online

Keywords:

Aerated gasification

Two-compartment fluidized bed

Internally circulating fluidized bed gasifier

Biomass gasification

Biomass energy

ABSTRACT

This study aims to improve the heating value (HV) of gas produced during the gasification of sawdust using a new type of air-blown gasifier based on a two-compartment cylindrical fluidized bed. The gasification process is based on an internally circulating aerated fluidized bed (ICAFB) and consists of two individual zones; a gasification zone in the annulus and combustion zone in the draft tube. The annulus and draft tube are connected via orifices at the lower section of the draft tube wall to enable the solids to move from the annulus to the draft tube. Char, gasified residue, together with hot bed material move to the draft tube and combust to produce heat. Fluidization ratio (R_Q) which is the ratio of air flow rate in the annulus (Q_{an}) to the air flow rate in the draft tube (Q_{dt}) together with equivalence ratio (ER) were used to control the temperature of the gasifier. The effects of ER on the temperature system stabilization, composition, HV of producer gas (PG) and gasifier performance were presented. ER ranges from 0.148 to 0.203 were used in this study. PG compositions of 3.13%, 2.28%, 25.8%, 8.2% and 22.48% for H_2 , O_2 , CO, CH_4 and CO_2 respectively with a HV of about 6.96 MJ m^{-3} were obtained at an ER of 0.185 and temperature of about 866°C . Compared with previous air-blown fluidized bed biomass gasification results, the ICAFB gasifier is capable of producing producer gas with higher CO and CH_4 fractions.

© 2015 Elsevier Ltd. All rights reserved.

1. Introduction

Global energy needs in the future will continue to increase, whilst primary energy sources from fossil continue to decline. Amongst renewable energy sources like solar, wind, wave and geothermal, energy from biomass is a potential energy source due to its abundant supply to complement the present fuel

mix [1]. Biomass can be converted into gaseous fuel and chemical products through the gasification process [2]. Gaseous fuel is conveniently used in both internal and external combustion engines or in furnaces for steam generation to produce electricity [3].

Studies have been conducted on biomass gasification with different gasifier designs, gasifying medium, fluidization

* Corresponding author. Tel.: +60 4 5937788; fax: +60 4 5941025.

E-mail address: mezainal@eng.usm.my (Z.A. Zainal).

<http://dx.doi.org/10.1016/j.biombioe.2015.03.023>

0961-9534/© 2015 Elsevier Ltd. All rights reserved.

List of symbol

D_{dt}	draft tube diameter, mm
D_{or}	orifice diameter, mm
ER	equivalence ratio
G_s	solid circulation rate, kg h^{-1}
H_{dt}	draft tube height, mm
H_{bs}	bed static height, mm
HV	heating value, MJ m^{-3}
Q_{an}	aeration flow rate, L m^{-1}
Q_{dt}	fluidization flow rate, L m^{-1}
RQ	fluidization rate
W_f	feed rate, kg h^{-1}

regimes and using catalysts to meet the desired final products [4–13]. Most of the gasifiers burn part of the biomass with limited air as the gasification agent, resulting in low heating values of $3.5\text{--}5 \text{ MJ m}^{-3}$ [12]. This is due to the high concentration of nitrogen in the air that causes dilution of the producer gas (PG). For this reason, steam is used instead of air to avoid dilution and to improve the heating value (HV) of the PG. The gasification process using steam or oxygen as the gasifying agent is able to produce a medium heating value gas of $10\text{--}18 \text{ MJ m}^{-3}$ [13,17,19]. However, both steam and oxygen gasification systems consume considerable amounts of energy. In addition, air-blown gasification has a lower tar content compared to steam-blown or steam-oxygen gasification [17].

The operating temperature in a fluidized bed gasifier is normally maintained by using devices such as an electric furnace as external heat sources, and also by burning part of the PG using secondary air at the freeboard of the reactor [22]. In most fluidized bed biomass gasification studies, the temperature is maintained by using air as the gasification agent. Increasing the amount of air increases the rate of the exothermic reactions which releases energy and, thus, increases the temperature [23]. Usually a fluidized bed gasifier is operated with an equivalence ratio (ER) varying from 0.20 to 0.45 resulting in heating values of $4.5\text{--}5.7 \text{ MJ m}^{-3}$ [4–10,24–26]. Lower ER than 0.18 would not be able to sustain gasification in the gasifier whilst ER higher than 0.45 produces high CO_2 instead of combustible gas [8].

The economic potential of the gasification process can be increased by burning some of the char byproduct in a separate zone to provide heat for the gasification process. For char burning, dual fluidized beds (DFB) and internally circulating fluidized beds (ICFB) have been developed [27,28]. Studies of ICFB on cold model experiments used a centrally located riser tube in an annular downcomer, where the particle travels downward and a connecting port at the bottom wall of the riser tube allows the particles to move from the annular downcomer into the riser tube [29]. Some of the ICFB have been used for coal gasification [29,30] and coal combustion [31–33]. However, most of them used steam as the gasifying agent with an additional heat supply to sustain the operating temperature of the system.

An internally circulating aerated fluidized bed (ICAFB) is an indirect heated pyrolysis process, where the energy needed

for gasification is provided by heat transfer from a combustion zone through bed material circulation and heat transfer due to direct contact between the combustion and the gasification zones. The advantage of this reactor to ICFB is that the combustion zone operates in the vigorous bubbling regime with restricted aeration in the gasification zone. Biomass is directly fed into the gasification zone, whilst the char (gasification product) moves into the combustion zone. The term “aeration” is used to describe the fluidization regime in the gasification zone which is below the minimum fluidization condition [34]. The basic principle of ICAFB is shown in Fig. 1.

In this work the ICAFB gasifier is constructed of two concentric cylinders. The inner cylinder (draft tube) acts as a combustion zone or heat generator providing heat to the annulus that acts as a gasification zone. Aeration in the annulus is needed to ensure the circulation of the bed particles between the annulus and the draft tube and to purge the gasification gaseous product from the annulus. Solid circulation rate (G_s) between the annulus and the draft tube is an important parameter to determine the overall performance of the ICAFB system.

2. Methodology

2.1. System setup

The gasifier is based on ICAFB with a total height of 1.1 m consisting of two parts: an annulus (gasification zone) with a diameter of 0.3 m and a draft tube (combustion zone) with a height of 0.32 m and diameter of 0.1 m. The two zones are connected via orifices at the lower section of the draft tube to enable the solids to move from the annulus to the draft tube. Eight equally spaced 0.02 m diameter holes were drilled in the wall of the draft tube, 0.08 m above its base. The ICAFB system is shown in Fig. 2.

The biomass (sawdust) is fed directly to the annulus from the top of the reactor. Char a byproduct of the gasification process and the bed material moves toward the draft tube via the orifice. A dipleg is installed to separate the flue gas and the producer gas. The bed material overflow from the top of the draft tube to the annulus and the flue gas passes through the dipleg and enters the cyclone separator. The axial temperature in the bed was measured using three K-type thermocouples mounted along the bed height from the distributor. The air chamber comprises of two plenums to separately supply fluidization air into the draft tube (Q_{dt}) and aerated air into the annulus (Q_{an}). The draft tube air supply consists of a distributor plate with seven bubble caps, whilst the annulus has a 60° conical base with 18 bubble caps.

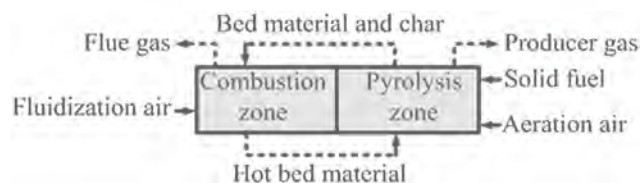


Fig. 1 – Principle of ICAFB.

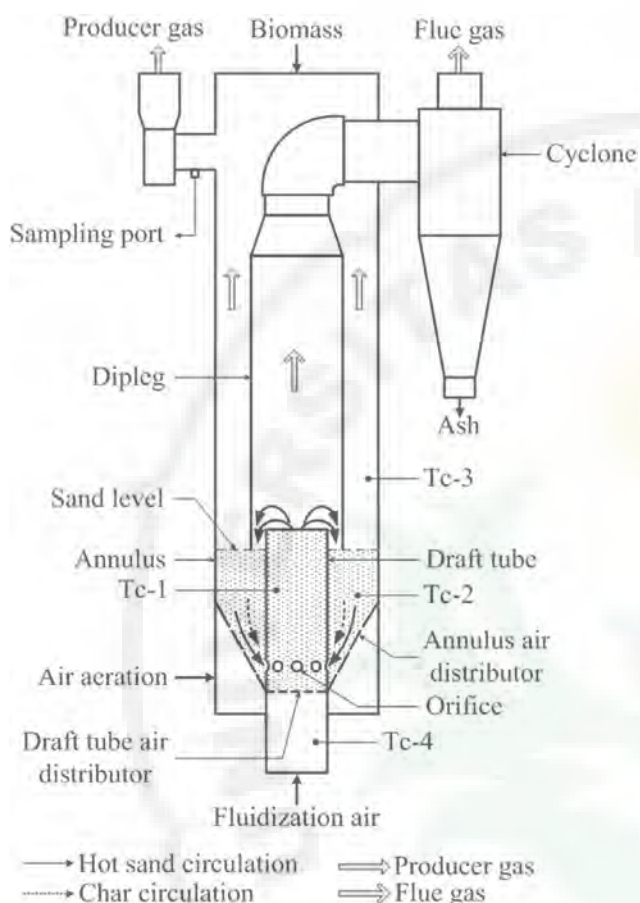


Fig. 2 – Schematic diagram of the ICAFB.

Sawdust is fed from the top of the reactor through a screw feeder connected to a sawdust hopper. Since sawdust gasification takes place in the annulus, sawdust is fed from the top of the reactor to provide a longer residence time before the sawdust becomes char and enters the combustor. A cyclone (0.20 m i.d. and 0.43 m high) is installed at the outlet of the draft tube. There are particulates in the producer gas from the annulus region. But since the flow rate at exit of the annulus is low, cyclone separator would not be an effective mean to remove any particulate present in the producer gas. The particulate present can be removed by other filtration system. The effects of equivalence ratio (ER) on the temperature system stabilization, composition, and heating value of producer gas were studied. The ER was adjusted by controlling the air flow rate into the annulus while the air flow rate into the draft tube was held constant.

2.2. Material and preparations

2.2.1. Bed material

The bed material is sand, with a mean particle size of 425–600 μm and a density of 1520 kg m^{-3} , belonging to Geldart Group B particles. The static bed height in the annulus and the draft tube were maintained at 0.28 m. The bed was fluidized with air provided from a blower. The pressure drop across the

draft tube is measured by a digital manometer through two pressure tappings, one at the disengaging zone and the other before the air distribution plate. Different air flow rate was performed in the draft tube and the annulus to induce circulation of the bed material between the draft tube and the annulus. Q_{dt} is set 350 L m^{-1} , which is about 2.33 times of the minimum fluidization flow rate ($Q_{mf} = 150 \text{ L m}^{-1}$), while the Q_{an} is set to 33%, 66%, 100% and 133% of the Q_{mf} . G_s is an important parameter for heat transfer and to control the gasification zone temperature. Measurement of G_s was carried out experimentally using hydrodynamic studies. The solid circulation rate was determined by collecting solids emerging from the top of the draft tube for a known interval of time and weighing to obtain the circulation rate.

2.2.2. Biomass material

Biomass material is sawdust obtained from local Malaysian rubber wood furniture home industries. Size distribution, ultimate and proximate analysis of the sawdust are presented in Tables 1 and 2 respectively.

The sawdust feeding system consists of a hopper and a screw feeder with a variable speed drive (VSD). The screw feeder was calibrated to determine the sawdust load capacity or feed rate (W_f) through the feeding system. The average sawdust flow rate is plotted against the screw feeder operating frequency as shown in Fig. 3.

2.3. Equivalence ratio calculation

For any process that involving biomass gasification, ER is used to quantify the proximity of a mixture (biomass + air) to its combustion stoichiometric conditions. In this work, ER was calculated based on both air flow rates into both the gasification and combustion zones. The following equation (1) is used to calculate the ER.

$$ER = \frac{(A/F)_{\text{actual}}}{(A/F)_{\text{stoichiometry}}} \quad (1)$$

where $(A/F)_{\text{actual}}$ is the actual gasification air fuel ratio into the gasifier, whilst $(A/F)_{\text{stoichiometry}}$ is the stoichiometric air fuel ratio.

2.4. Start-up method

An important aspect of the operation of the gasifier is the start-up process. The combustor was initially heated, using liquid petroleum gas (LPG). At the start of the experiment, air

Table 1 – Size distribution of sawdust.

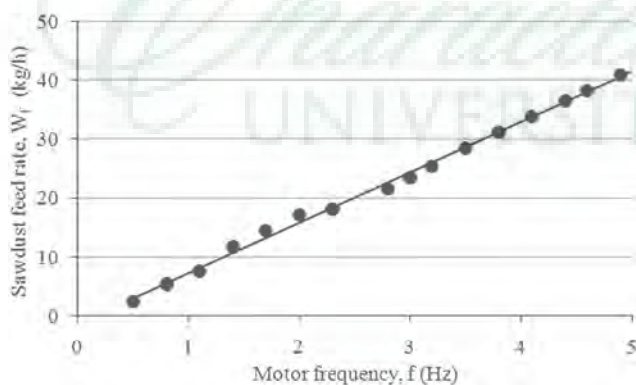
Size (mm)	Weight (%)
S > 1.7–2.0	2.24
1.17–1.70	2.60
0.6–1.17	76.40
0.5–0.6	5.32
0.425–0.5	3.64
0.3–0.425	5.20
S < 0.3	4.6
Sum	100.00

Table 2 – Ultimate and proximate analysis of sawdust.

Ultimate and proximate analyses of sawdust	
Ultimate analysis, wt.% (air dry basis)	
C	50.54
H	7.08
O	41.11
N	0.15
S	0.57
Proximate analysis, wt.% (air dry basis)	
Volatiles	82.29
Fixed carbon	17.16
Moisture	8.0
Ash	0.55
Heating value (dry basis)	
Low heating value (MJ/kg)	15.00

was supplied to the draft tube at 200 L min^{-1} with LPG at 20 L min^{-1} . The air and LPG mixture was ignited using a spark plug. The hot gas fluidizes the sand and increases the bed temperature. Temperatures at the annulus and the draft tube were recorded using type K thermocouples. A thermocouple was also installed at the air-LPG combustor chamber to detect combustion during start-up process.

The difference between the annulus and the draft tube air flow rates promotes solid circulation from the two zones through the connecting orifices. Circulation of the bed material from the draft tube to the annulus provides heat transfer from the combustion zone to the gasification zone. When the bed temperature in the annulus reached $400 \text{ }^\circ\text{C}$ (Tc-2), sawdust was fed into the annulus. The sawdust starts to pyrolyze and converts into volatiles and char. The char together with sand move under gravity, flow into the draft tube and are burnt to produce heat with excess air. When the temperature of draft tube reached $650\text{--}700 \text{ }^\circ\text{C}$ (Tc-1), the LPG was switched-off and the experimental parameter was adjusted to the desired value based on R_Q and ER. The heat produced by the char combustion in the draft tube further increases the temperature to the desired level. After 40 min at which time the gasifier operation reached a steady state, gas samples were collected. Temperatures at various points of the system, the aerated, and the fluidization air flow were recorded and controlled.

**Fig. 3 – Screw feeder calibration.**

2.5. Producer gas sampling and analysis

A small portion of the PG was collected using a gas sampling train that removes any moisture and particulates present in the PG before being used in a TCD gas chromatograph equipped with Carboxene 1000 (Supelco, USA) column ($15 \text{ f} \times 1/8 \text{ in}$, 80/100 mesh) for determination of the gas composition.

3. Results and discussion

In this work, the discussion is focused on the results obtained from the optimum experimental operating conditions as shown in Table 3.

3.1. Solid circulation rate (G_s)

Solid circulation rate was measured based on isothermal experiment. Fig. 4 shows the dependence of G_s on R_Q . Initially G_s is low because Q_{an} is much smaller than Q_{mf} . Consequently the bed material in the annulus is packed more densely and enters the draft tube slowly. However, G_s increases by increasing R_Q due to the active movement of the solid particles. The diluted density of the annulus bed decreases, thus leading to easier solid movement into the draft tube and consequently an increase in G_s .

G_s then decreases when R_Q is greater than 0.43 where bubbles start to form in the annulus which leads to a decrease in the bed density. A higher Q_{an} causes a reduction in the bed density and pressure difference (ΔP) between the annulus near the orifice, which results in a lower G_s . The optimum value of G_s was found at $R_Q = 0.43$.

3.2. Temperature stabilization

Fig. 5 shows the temperature profile of the system at $R_Q = 0.43$ and ER = 0.185. Once the temperature in the draft tube reaches approximately $700 \text{ }^\circ\text{C}$, the LPG was turned-off. The temperature of the LPG combustion chamber (Tc-4) decreases sharply, but the temperature of the draft tube bed continue to increase to a stable limit, approximately $866 \text{ }^\circ\text{C}$.

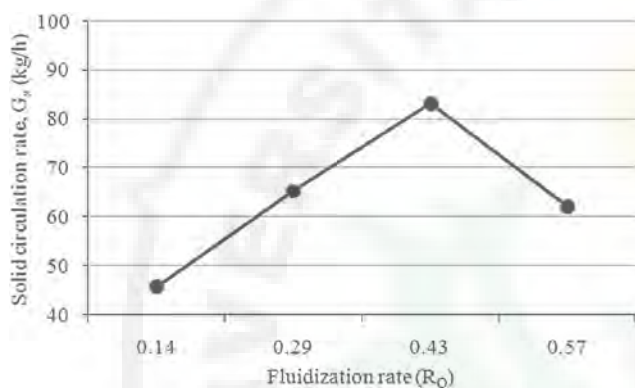
The temperatures of the annulus bed (Tc-2) and annulus freeboard (Tc-3) depend on Tc-1 and R_Q . The heat produced during the char combustion process in the draft tube is immediately transferred to the annulus by the bed material circulation. The system reached steady state in a reaction time of 15 min after sawdust was fed into the gasifier. The average temperature in the draft tube is about $66 \text{ }^\circ\text{C}$ higher than the annulus. This means that the circulating bed material transports heat from the combustion to the annulus. Tc-3, which is 20 cm above the static bed height was nearly constant at approximately $500 \text{ }^\circ\text{C}$.

3.3. Effect of equivalence ratio (ER) on the bed temperature

Bed temperature affects the chemical reactions in the gasification process. In this work, the operating temperature is controlled through the ER by varying R_Q at constant W_f . The range of ER used in this work was 0.148–0.203 which was

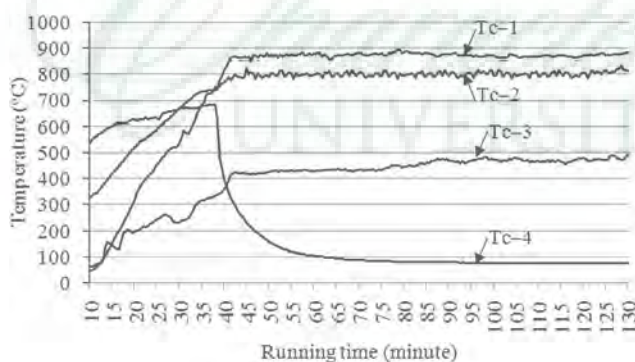
Table 3 – Results from the optimum condition.

No. run	Q_{dt} (L m ⁻¹)	Q_{an} (L m ⁻¹)	G_s (kg h ⁻¹)	W_f (kg h ⁻¹)	T_{dt} (°C)	T_{an} (°C)	Gas composition (vol.%)						HV (MJ m ⁻³)
							H ₂	O ₂	CO	CH ₄	CO ₂	N ₂	
1	350	50	53.73	31.18	822	747	2.45	1.10	20.64	4.96	18.13	52.61	4.89
2		100	74.22		845	778	2.68	1.18	23.41	5.80	19.28	47.43	5.82
3		150	86.59		866	806	3.13	2.28	25.80	8.20	22.48	38.11	6.92
4		200	70.10		838	764	3.11	1.37	23.98	5.82	21.49	43.60	5.61

**Fig. 4 – Effect of R_Q on G_s .**

slightly below the ER for normal fluidized bed gasifier (0.20–0.40) [12]. However, in the ICAFB gasifier, an ER lower than 0.20 could be used, because the most important parameter is G_s , which is highly dependent on R_Q . Fig. 6 illustrates the effect of ER on the operating temperatures of the draft tube (Tc-1) and the annulus (Tc-2). The increase in temperature with ER is well understood because ER increases with R_Q . By increasing R_Q at a constant W_f , ER increases as well as G_s and thus the amount of char released from the annulus to the draft tube also increases.

Increasing char formation in the annulus increases its flow into the draft tube resulting in higher heat production during the combustion process. But there is an optimum limit that should not be exceeded else it would lead to two effects: 1. The temperature inside the annulus becomes uncontrollable or overheats; 2. Char accumulates in the annulus because gas

**Fig. 5 – Temperature profile of the system during in operation.**

production is not balanced with feeding, resulting in an impaired gasification process.

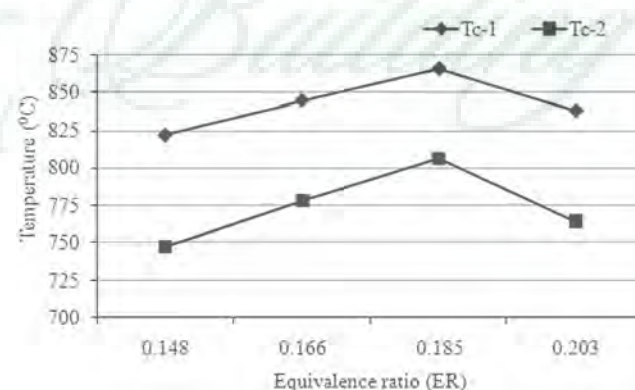
Increasing R_Q further leads to an increase in ER, but decrease in G_s . This causes the whole temperature to decrease. It was also found that for Q_{dt} either below or above 350 L min⁻¹, the temperature of the whole system gradually decreases. Below 350 L min⁻¹, G_s is low and causes insufficient char transfer to the draft tube for heat generation. Above 350 L min⁻¹ however the fluidization regime becomes vigorous, causing some of the char to elutriate from the draft tube, and thus reducing heat generation during combustion. Therefore Q_{dt} is maintained constant at 350 L min⁻¹ for all tests in this work.

In this study, the gasification operating temperature in the gasification zone that can be achieved was in the range 747–806 °C. This temperature range is categorized in the intermediate temperature gasification where the major product is gas [35,36]. This temperature is sufficient for char reaction with reactive gases such as O₂, H₂ and CO₂.

From Fig. 6, the highest combustion temperature was found to be approximately 866 °C. This is an important issue in the design of fluidized bed combustor, because typical fluidized bed furnaces operate at 800–900 °C to avoid fouling and NO_x [37]. However, high combustion temperature (900–1100 °C) contribute to better combustion efficiency where carbon fines are burnt completely before they escape from the combustor through the cyclone.

3.4. Producer gas composition and heating value

Several researchers examined the composition and heating value of product gas with respect to the operating temperature at constant ER. However in this work the temperature is varied with ER. Increasing ER causes the temperature to rise and also

**Fig. 6 – Effect of ER on temperature.**

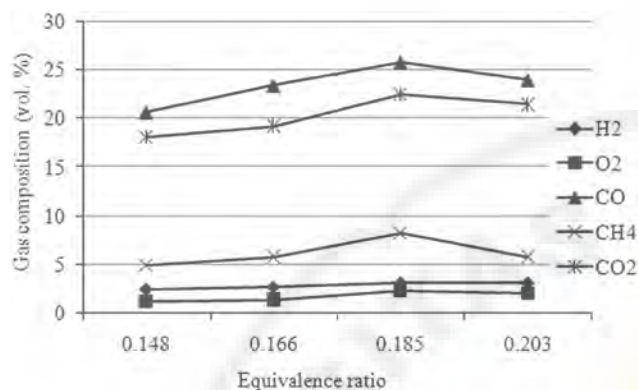


Fig. 7 – Producer gas composition.

increases the rate of chemical reactions. Fig. 7 shows the variation in the producer gas composition from the annulus with respect to ER.

Fig. 7 indicates the optimum operating condition at an ER of 0.185 producing gas compositions of 3.13%, 2.28%, 25.8%, 8.2% and 22.48% for H₂, O₂, CO, CH₄ and CO₂ respectively. Carbon monoxide and methane are the largest constituents of the producer gas, and are much higher than typically found from air-blown fluidized bed gasification as described in Table 4. Comparison of the ICAFB gasifier shows the improvement to the other types of gasifiers in terms of producer gas quality. The separate gasification and combustion compartment reduces the dilution of the producer gas with excessive N₂. The performance of the gasifier would be greatly improved with steam injection.

Increasing the ER from 0.148 to 0.185 increases reaction temperature in the gasification zone. The CO content increases significantly when the temperature in the gasification zone increases from 747 to 806 °C. Furthermore, pyrolysis process and subsequent thermal cracking of vapor could also contribute to the increase in the CO content.

However, by increasing the ER further (ER = 0.203), the gasification temperature considerably decreases. Higher ER causes low concentrations of producer gas constituent due to increase oxidation/combustion of char and product gas [7]. In an ordinary fluidized bed gasifier, the CO productions still continue to increase at temperature beyond 820 °C at a constant ER [8,9]. In this work, the CO concentration of the producer gas markedly increases from 20.64% to 25.80% in the investigated ER range. However, increasing the ER further causes the temperature of gasifier to decrease due to decrease in the solid circulation rate inside the gasifier and causes reduction in CO content.

It also can be seen from Fig. 7 that the concentration of H₂ does not vary very much. It was found that the highest H₂ content was 3.13%. This is low compared to common air-blown fluidized bed gasification [4–6,8–11]. This is due to the effect of the gasification reaction temperature where the gasification temperature in this work was lower than the other authors. The composition of H₂ is very dependent on the reaction temperature and the gasification agent used [14,16]. Several researchers added steam to the gasifier in order to increase the H₂ production [13,15,17–21]. A high gasification temperature (800–1000 °C) favors thermal cracking of the hydrocarbons and thus sharply increases the yield of H₂ through water-gas and steam reforming reactions [16,21,38–40]. However, in this study the gasification reaction temperature is limited to a maximum of 806 °C resulting in low H₂ yield.

The methane composition in this study was very high as compared to other authors [4–6,8–11] which may have been due to the much lower temperature of our gasifier bed during these experiments. Higher temperature tends to favor steam reforming of methane which decreases the concentration of methane and increases the concentration of hydrogen [16,17]. It is well known that air gasification produces high CO₂ concentration [18]. In this work, the CO₂ content increases with ER which is similar to the other researcher [7–9]. This CO₂ level will continue to increase with ER as the combustion reaction increase cause the quality of the product gas decrease.

Table 4 – Comparison of producer gas produced by air-blown ICAFB.

Gasifier type	ER	Temp (°C)	Fuel constituent (vol.%)					HV (MJ m ⁻³)	Ref.
			H ₂	CO	CH ₄	CO ₂	N ₂		
Cyclone	0.19–0.53	700	16	10	n.a	30	n.a	3.90	[4]
Cyclone	0.23–0.35	733–835	7.5	27	3.5	7.5	n.a	5.7	[5]
Entrained	0.22–0.34	700–1000	14.6	25.71	2.45	12	n.a	6.67	[6]
BFB	0.20–0.45	750–850	9.5	18	4.5	13.5	n.a	6.3	[8]
BFB	0.17–0.32	650–1050	19.5	17.5	2.5	13.75	n.a	5.88	[9]
Two-stage FB	0.20–0.45	750–950	9.27	9.25	4.21	13.28	n.a	5	[10]
Entrained	n.a	1050	7	16	3	18	n.a	5	[11]
BFB	0.17–0.23	718–733	n.a	n.a	n.a	n.a	n.a	4.74	[12]
BFB	0.25–0.35	665–830	4.0	19.9	2.9	14.45	56.57	5.03	[23]
BFB	0.2–0.4	758–850	23.98	14.26	3.75	19.42	n.a	6.54	[43]
BFB	0.18–0.27	610–810	5–8	16–21	4–6	15–16	n.a	6.40	[44]
BFB	0.3–0.46	750–880	7–15	10–20	2–10	14–23	n.a	4–8	[45]
ICAFB	0.148–0.203	747–806	3.13	25.80	8.20	22.48	38.11	6.96	[*]

[*] Current work.

n.a: not available.

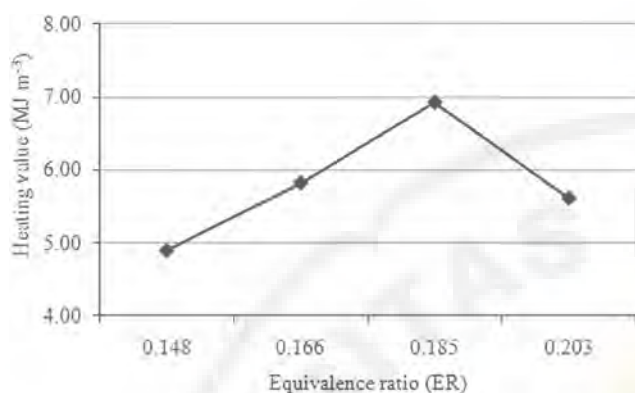


Fig. 8 – Effect of equivalence ratio on heating value.

Fig. 8 shows the heating value of the producer gas. The heating value increases with an increase in ER due to the increase in the percentages of CO and CH₄. The highest heating value of the producer gas was an average of 6.96 MJ m⁻³.

3.5. Gasifier's performance

Mass and energy balances in the ICAFB gasifier were calculated to determine the performance of the gasifier as well as the carbon conversion and thermal efficiency (cold gas efficiency). Dry gas yield was calculated by using equation (2) [38].

$$Y = \frac{Q_a \times 0.79}{W_f(1 - X_{\text{ash}}) \times N_2\%} \quad (2)$$

where Q_a is the flow rate of air into annulus (Nm³ h⁻¹), W_f is the mass flow rate of biomass (kg h⁻¹), X_{ash} is the ash content in the feed and $N_2\%$ is the volumetric percentage of N₂ in the dry producer gas. The carbon conversion is calculated on the basis of volumetric percentages of CO, CO₂ and CH₄ in the producer gas as shown in equation (3) [38].

$$\eta_c = \frac{Y(\text{CO}\% + \text{CH}_4\% + \text{CO}_2\%) \times 12}{22.4 \times \text{C}\%} \times 100\% \quad (3)$$

where C% is the mass percentage of carbon in the feed obtained from the ultimate analysis of biomass. Cold gas efficiency which is percentage of the biomass heating value converted into heating value of the producer gas is calculated by using equation (4) [38].

$$\eta_{\text{cg}} = \frac{H_g \times Y}{H_b \times W_f} \times 100\% \quad (4)$$

where H_g (MJ N⁻¹ m⁻³) and H_b (MJ kg⁻¹) represent the heating value of the producer gas and biomass respectively.

The mass balance was found to 83.37%. This is slightly low due to some of the ash from the draft tube was not captured by the cyclone separator. The value of mass balance closure should be in the ranges of 90–95% [41]. Higher heating value of producer gas compared to conventional fluidized bed gasifier is the advantage of ICAFB gasifier. However, energy balance achieved was 65.5% which is below the recommended ranges value 80–85% [42]. This is due to the difficulty in determining the heat loss from the gasifier and cyclone separator walls that

were covered by asbestos blanket. Heat from complete char combustion might not be transported properly from combustion into gasification zones. The gas yield, carbon conversion and cold gas efficiency obtained from the optimum conditions were 1.29 Nm³ h⁻¹, 70.94%, and 54.67% respectively.

4. Conclusions

A pilot-scale of a new type gasifier with two-compartment cylindrical based on internally circulating aerated fluidized bed (ICAFB) has been successfully developed. The most important parameters in the ICAFB are the fluidization ratio (R_Q) that controls the solid circulation rate (G_s) and the ER in the gasifier. Circulation of the bed material from annulus to draft tube is the most important parameter and determines the heat transfer from the combustion zone to the gasification zone.

This study indicates that under the optimum operating conditions at an ER of 0.185 and gasification temperature of about 806 °C, producer gas compositions of 3.13%, 2.28%, 25.8%, 8.2% and 22.48% for H₂, O₂, CO, CH₄ and CO₂ respectively with a heating value of about 6.96 MJ m⁻³ was achieved. Significant amounts of carbon monoxide (CO) and methane (CH₄) were produced at an intermediate operating temperature of about 806 °C, where the reactions favor the production of CO and CH₄.

Acknowledgment

The financial support provided by Research University Grant No. 1001/814159 of the Universiti Sains Malaysia is gratefully acknowledged.

REFERENCES

- [1] Balat M. Biomass energy and biochemical conversion processing for fuels and chemicals. *Energy Sources Part A Recovery Util Environ Eff* 2006;28(6):517–25.
- [2] Saxena RC, Seal D, Kumar S, Goyal HB. Thermo-chemical routes for hydrogen rich gas from biomass: a review. *Renew Sustain Energy Rev* 2008;12(7):1909–27.
- [3] Demirbas A. Biomass gasification for power generation in Turkey. *Energy Sources Part A Recovery Util Environ Eff* 2006;28(5):433–45.
- [4] Miskam MA, Zainal ZA, Idroas MY. Performance and characteristics of a cyclone gasifier for gasification of sawdust. *J Appl Sci* 2008;8(1):95–103.
- [5] Gao J, Zhao Y, Sun S, Che H, Zhao G, Wu J. Experiments and numerical simulation of sawdust gasification in an air cyclone gasifier. *Chem Eng J* 2012;213:97–103.
- [6] Zhao Y, Sun S, Zhou H, Sun R, Tian H, Luan J, et al. Experimental study on sawdust air gasification in an entrained-flow reactor. *Fuel Process Technol* 2010;91(8):910–4.
- [7] Radmanesh R, Chaouki J, Guy C. Biomass gasification in a bubbling fluidized bed reactor: experiments and modeling. *AIChE J* 2006;52(12):4258–72.
- [8] Narvaez I, Orío A, Aznar MP, Corella J. Biomass gasification with air in an atmospheric bubbling fluidized bed. Effect of

- six operational variables on the quality of the produced raw gas. *Ind Eng Chem Res* 1996;35(7):2110–20.
- [9] Lahijani P, Zainal ZA. Gasification of palm empty fruit bunch in a bubbling fluidized bed: a performance and agglomeration study. *Bioresour Technol* 2011;102(2):2068–76.
- [10] Cao Y, Wang Y, Riley JT, Pan W-P. A novel biomass air gasification process for producing tar-free higher heating value fuel gas. *Fuel Process Technol* 2006;87(4):343–53.
- [11] Hernandez JJ, Aranda-Almansa G, Bula A. Gasification of biomass wastes in an entrained flow gasifier: effect of the particle size and the residence time. *Fuel Process Technol* 2010;91(6):681–92.
- [12] Lim MT, Alimuddin Z. Bubbling fluidized bed biomass gasification—performance, process findings and energy analysis. *Renew Energy* 2008;33(10):2339–43.
- [13] Schuster G, Löffler G, Weigl K, Hofbauer H. Biomass steam gasification - an extensive parametric modeling study. *Bioresour Technol* 2001;77(1):71–9.
- [14] Asadullah M, Ito S-i, Kunimori K, Yamada M, Tomishige K. Biomass gasification to hydrogen and syngas at low temperature: novel catalytic system using fluidized-bed reactor. *J Catal* 2002;208(2):255–9.
- [15] Boateng A, Walawender W, Fan L, Chee C. Fluidized-bed steam gasification of rice hull. *Bioresour Technol* 1992;40(3):235–9.
- [16] Turn S, Kinoshita C, Zhang Z, Ishimura D, Zhou J. An experimental investigation of hydrogen production from biomass gasification. *Int J Hydrog Energy* 1998;23(8):641–8.
- [17] Lv PM, Xiong ZH, Chang J, Wu CZ, Chen Y, Zhu JX. An experimental study on biomass air-steam gasification in a fluidized bed. *Bioresour Technol* 2004;95(1):95–101.
- [18] Pinto F, Franco C, Andre RN, Tavares C, Dias M, Gulyurtlu I, et al. Effect of experimental conditions on co-gasification of coal, biomass and plastics wastes with air/steam mixtures in a fluidized bed system. *Fuel* 2003;82(15):1967–76.
- [19] Gil J, Aznar MP, Caballero MA, Frances E, Corella J. Biomass gasification in fluidized bed at pilot scale with steam-oxygen mixtures. Product distribution for very different operating conditions. *Energy Fuel* 1997;11(6):1109–18.
- [20] Li X, Grace J, Lim C, Watkinson A, Chen H, Kim J. Biomass gasification in a circulating fluidized bed. *Biomass Bioenergy* 2004;26(2):171–93.
- [21] Kumar A, Eskridge K, Jones DD, Hanna MA. Steam-air fluidized bed gasification of distillers grains: effects of steam to biomass ratio, equivalence ratio and gasification temperature. *Bioresour Technol* 2008;100(6):2062–8.
- [22] Cheng G, Li Q, Qi F, Xiao B, Liu S, Hu Z, et al. Allothermal gasification of biomass using micron size biomass as external heat source. *Bioresour Technol* 2012;107:471–5.
- [23] Mansaray K, Ghaly A, Al-Taweel A, Hamdullahpur F, Ugursal V. Air gasification of rice husk in a dual distributor type fluidized bed gasifier. *Biomass Bioenergy* 1999;17(4):315–32.
- [24] Tzeng LM, Zainal ZA. Operational investigation of a bubbling fluidized bed biomass gasification system. *Energy Sustain Dev* 2007;11(1):88–93.
- [25] Wang Y, Yoshikawa K, Namioka T, Hashimoto Y. Performance optimization of two-staged gasification system for woody biomass. *Fuel Process Technol* 2007;88(3):243–50.
- [26] Hurley S, Xu C, Preto F, Shao Y, Li H, Wang J, et al. Catalytic gasification of woody biomass in an air-blown fluidized-bed reactor using Canadian limonite iron ore as the bed material. *Fuel* 2012;91(1):170–6.
- [27] Xiao X, Le DD, Morishita K, Zhang S, Li L, Takarada T. Multi-stage biomass gasification in internally circulating fluidized-bed gasifier (ICFG): test operation of animal-waste-derived biomass and parametric investigation at low temperature. *Fuel Process Technol* 2010;91(8):895–902.
- [28] Zhang H, Xiao R, Wang D, Cho J, He G, Shao S, et al. Hydrodynamics of a novel biomass autothermal fast pyrolysis reactor: solid circulation rate and gas bypassing. *Chem Eng J* 2012;181–182:685–93.
- [29] Kim YJ, Lee JM, Kim SD. Coal gasification characteristics in an internally circulating fluidized bed with draught tube. *Fuel* 1997;76(11):1067–73.
- [30] Lee J, Kim Y, Kim S. Catalytic coal gasification in an internally circulating fluidized bed reactor with draft tube. *Appl Therm Eng* 1998;18(11):1013–24.
- [31] Roh SA, Jung DS, Kim SD, Guy C. Combustion characteristics of spent catalyst and paper sludge in an internally circulating fluidized-bed combustor. *J Air Waste Manag Assoc* 2005;55(9):1269–76.
- [32] Lee WJ, Cho YJ, Kim JR, Kim SD. Coal combustion characteristics in a fluidized bed combustor with a draft tube. *Korean J Chem Eng* 1992;9(4):206–11.
- [33] Jeon JH, Kim SD, Kim SJ, Kang Y. Combustion and heat transfer characteristics in a square internally circulating fluidized bed combustor with draft tube. *Fuel* 2008;87(17–18):3710–3.
- [34] Nam CH, Pfeffer R, Dave RN, Sundaresan S. Aerated vibrofluidization of silica nanoparticles. *AIChE J* 2004;50(8):1776–85.
- [35] Chen G, Leung DYC. Experimental investigation of biomass waste, (rice straw, cotton stalk, and pine sawdust), pyrolysis characteristics. *Energy Sources* 2003;25(4):331–7.
- [36] Demirbas A. Pyrolysis mechanisms of biomass materials. *Energy Sources Part A Recovery Util Environ Eff* 2009;31(13):1186–93.
- [37] Basu P. *Combustion and gasification in fluidized beds*. CRC Press; 2006.
- [38] Xiao R, Zhang M, Jin B, Huang Y, Zhou H. High-temperature air/steambrown gasification of coal in a pressurized spout-fluid bed. *Energy Fuel* 2006;20:715–20.
- [39] Ghani WAWAK, Moghadam RA, Salleh MAM, Alias AB. Air gasification of agricultural waste in a fluidized bed gasifier: hydrogen production performance. *Energies* 2009;2(2):258–68.
- [40] Umeki K, Yamamoto K, Namioka T, Yoshikawa K. High temperature steam-only gasification of woody biomass. *Appl Energy* 2010;87(3):791–8.
- [41] Chern SM, Walawender WP, Fan LT. Mass and energy balance analyses of a downdraft gasifier. *Biomass* 1989;18:127–51.
- [42] Rao MS, Singh SP, Sodha MS, Dubey AK, Shyam M. Stoichiometric, mass, energy and exergy balance analysis of countercurrent fixed-bed gasification of post-consumer residues. *Biomass Bioenergy* 2004;27:155–71.
- [43] Skoulou V, Koufodimos G, Samaras Z, Zabaniotou A. Low temperature gasification of olive kernels in a 5-kW fluidized bed reactor for H₂-rich producer gas. *Int J Hydrogen Energy* 2008;33(22):6515–24.
- [44] Wu C-z, Yin X-l, Ma L-l, Zhou Z-q, Chen H-p. Operational characteristics of a 1.2-MW biomass gasification and power generation plant. *Biotechnol Adv* 2009;27(5):588–92.
- [45] Gil J, Corella J, Aznar M, Caballero M. Biomass gasification in atmospheric and bubbling fluidized bed: effect of the type of gasifying agent on the product distribution. *Biomass Bioenergy* 1999;17(5):389–403.